Supporting Information

Chizhikov et al. 10.1073/pnas.0910786107

SI Materials and Methods

BAC Recombination and Generation of *Lmx1a-Cre* Transgenic Mice. Mouse BAC RP22-296O24 was selected for modification. This BAC contains ≈200 kb of the *Lmx1a* locus, including the first three exons of *Lmx1a*, the last three exons of the proximal *Rxrg* gene, and all intergenic sequences. After the vector backbone LoxP site was replaced with an amp^R gene, BAC recombineering (1) was used to target an *eGFP-Cre* cassette (2) into the translation initiation codon of *Lmx1a*. The *Lmx1a-Cre* BAC transgenic CD1 lines were obtained by standard pronuclear injection by the Transgenic Mouse Core Facility of the University of Chicago. Transgenic mice were identified by PCR analysis of tail DNA. (Primers are available upon request.)

Mice. Mouse lines used in this study include $Lmx1a^{drJ}$ (*dreher*) (Jackson Laboratory), in which Lmx1a is inactivated by a missense mutation (3), $Atoh1^{lacZ}$ (4), *Gdf7-Cre* (5), and the *Rosa26 LacZ* reporter strain (6) (Jackson Laboratories). All animal procedures conformed to the policies of the University of Chicago and to the National Institutes of Health guidelines on the care and use of laboratory animals and are in accordance with the applicable portions of the Animal Welfare Act.

Tissue Analysis. Immunohistochemistry was performed as previously described (7). Embryos were collected in cold PBS, fixed in cold 4% paraformaldehyde for 2–3 h, washed three times in PBS, sunk in 30% sucrose in PBS, and embedded in optimum cutting temperature (OCT) compound. Blocks of OCT compound were sectioned on a cryostat (12 μm). Sections were blocked with 5% serum in PBS and then incubated overnight at 4 °C with primary antibodies. Secondary antibodies were applied for 1 h at room temperature. We used the following primary antibodies: rabbit (1:500) (provided by M. German, University of California, San Francisco) and goat (1:200) (Santa Cruz Biotechnology) anti-Lmx1a antibodies, rabbit (1:300) (8) and mouse (1:5) (Studies Hybridoma Bank, University of Iowa) anti-Atoh1 antibodies, rabbit anti-Lhx2/9 antibody (1:1,000) (9), rabbit anti-Lhx2 antibody (1:200) (10), chicken anti-GFP antibody (1:300) (Abcam), rat anti-β-Galactosidase antibody (1:300) (11), mouse anti-Nestin antibody (1:150) (Chemicon), mouse anti-p73 antibody (1:50) (NeoMarkers), and rabbit anti-Tbr2 antibody (1:2,000) (12) together with the appropriate secondary antibodies (Invitrogen). In situ hybridization was performed as described (7), using digoxigenin-labeled riboprobes, alkaline phosphatase-conjugated anti-digoxigenin Fab fragments, and nitro blue tetrazolium/5-bromo-4-chloro-3-indolyl phosphate (NBT/BCIP) substrates. X-Gal staining, histology, BrdU labeling, and TUNEL assays were performed as described previously (7, 13).

Organotypic Slice Cocultures. All manipulations were performed as described previously (14, 15). Coculture experiments used tissue from embryonic day (e) 12.75 wild-type nontransgenic host embryos and age-matched wild-type and *dreher* donor embryos carrying the *Lmx1a-cre/ROSA* fate-mapping alleles. Briefly, embryos were collected into cold Krebs' buffer. The forebrains were discarded, and midbrain-hindbrain blocks were trimmed to include only cerebellum and adjacent brainstem. The tissue blocks were embedded in 4% low-melting agarose and sliced sagittally on a vibratome (300 μm). Slices from wild-type nontransgenic host brains were transferred to a Nucleopore polycarbonate membrane (Whatman). The wild-type RL was excised and replaced with equivalent RL tissue obtained from wild-type or *dreher Lmx1a-Cre/ROSA* donor tissue (Fig. 5*A*). Explants were cultured for 2 days in vitro on membranes floating on 10% FCS-supplemented culture medium (DMEM with glutamine and penicillin/streptomycin) in organ-culture plates at 37 °C with 5% CO_2. They then were fixed in 4% paraformaldehyde and processed for immunohistochemistry. In BrdU-labeling experiments, BrdU was provided 90 min before harvesting explants.

Data Analysis. At least three embryos, explants, or adult mice of each genotype (from two or more independent litters) were analyzed. ImageJ software (National Institutes of Health) was used to quantify the area of RL explants before and after cultivation. Quantitative data are expressed as the mean ± SD. Statistical significance was determined by two-tailed *t* test.

1. Lalioti M, Heath J (2001) A new method for generating point mutations in bacterial artificial chromosomes by homologous recombination in *Escherichia coli*. *Nucleic Acids Res* 29:E14.
2. Le Y, Miller JL, Sauer B (1999) GFPcre fusion vectors with enhanced expression. *Anal Biochem* 270:334–336.
3. Millonig JH, Millen KJ, Hatten ME (2000) The mouse Dreher gene *Lmx1a* controls formation of the roof plate in the vertebrate CNS. *Nature* 403:764–769.
4. Ben-Arie N, et al. (2000) Functional conservation of atonal and Math1 in the CNS and PNS. *Development* 127:1039–1048.
5. Lee KJ, Dietrich P, Jessell TM (2000) Genetic ablation reveals that the roof plate is essential for dorsal interneuron specification. *Nature* 403:734–740.
6. Soriano P (1999) Generalized lacZ expression with the ROSA26 Cre reporter strain. *Nat Genet* 21:70–71.
7. Chizhikov VV, Millen KJ (2004) Control of roof plate formation by Lmx1a in the developing spinal cord. *Development* 131:2693–2705.
8. Su HL, et al. (2006) Generation of cerebellar neuron precursors from embryonic stem cells. *Dev Biol* 290:287–296.
9. Lee KJ, Mendelsohn M, Jessell TM (1998) Neuronal patterning by BMPs: A requirement for GDF7 in the generation of a discrete class of commissural interneurons in the mouse spinal cord. *Genes Dev* 12:3394–3407.
10. Mangale VS, et al. (2008) Lhx2 selector activity specifies cortical identity and suppresses hippocampal organizer fate. *Science* 319:304–309.
11. Saul SM, et al. (2008) Math5 expression and function in the central auditory system. *Mol Cell Neurosci* 37:153–169.
12. Englund C, et al. (2005) Pax6, Tbr2, and Tbr1 are expressed sequentially by radial glia, intermediate progenitor cells, and postmitotic neurons in developing neocortex. *J Neurosci* 25:247–251.
13. Currle DS, Cheng X, Hsu CM, Monuki ES (2005) Direct and indirect roles of CNS dorsal midline cells in choroid plexus epithelia formation. *Development* 132:3549–3559.
14. Englund C, et al. (2006) Unipolar brush cells of the cerebellum are produced in the rhombic lip and migrate through developing white matter. *J Neurosci* 26:9184–9195.
15. Daza RA, Englund C, Hevner RF (2007) Organotypic slice culture of embryonic brain tissue. *Cold Spring Harb Protoc*, 10.1101/pdb.prot4914.

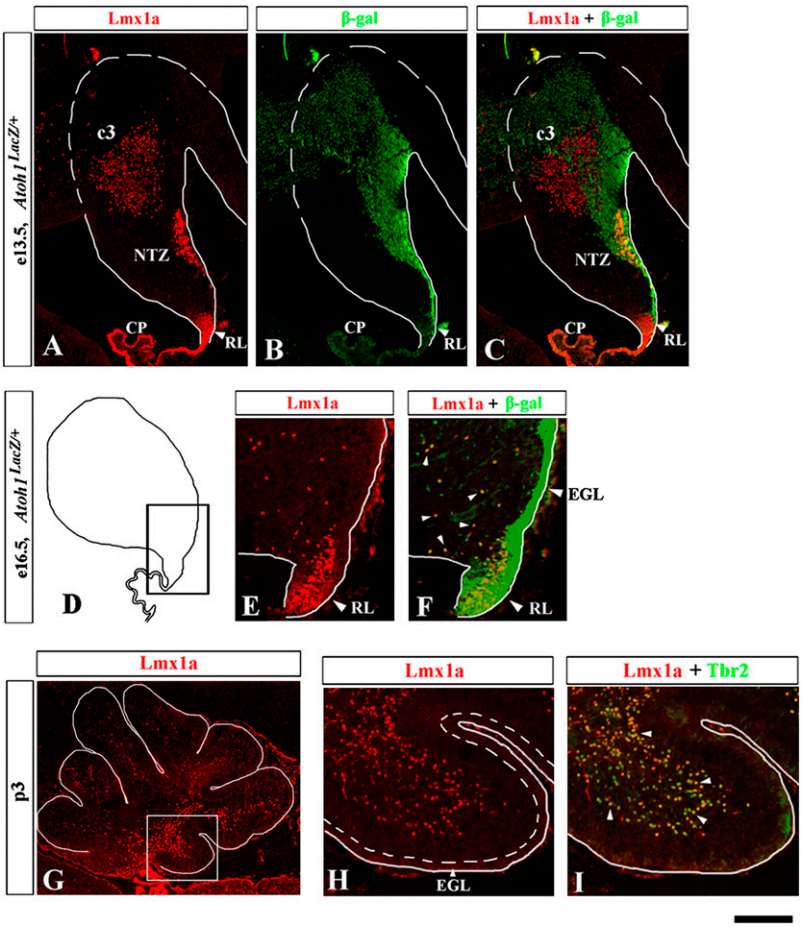

Fig. S1. Origin and identity of Lmx1a-expressing cells in the developing cerebellum. (*A*–*C*) Sagittal sections of e13.5 *Math1*$^{lacZ/+}$ embryos stained with Lmx1a (*A*), β-gal (*B*), or Lmx1a+ β-gal (*C*) antibodies. Choroid plexus (CP), rhombic lip (RL), and Lmx1a^{+} cells in nuclear transitory zone (NTZ) and c3 cells are indicated. NTZ cells coexpress Lmx1a and β-gal, indicating that they originate from Atoh1^{+} RL cells. c3 Cells are β-gal^{-}, indicating that they do not originate from Atoh^{+} RL cells. (*D*) Diagram of sagittal section of e16.5 cerebellar anlage. (*E* and *F*) Sagittal sections of e16.5 *Atoh1*$^{lacZ/+}$ cerebellum stained with anti-Lmx1a (*E*) or with anti-Lmx1a+ anti–β-gal (*F*) antibodies. The area shown corresponds to the boxed region in *D*. RL and external granule cell layer (EGL) are labeled. A group of Lmx1a^{+} cells originate from the Atoh1 lineage and migrate directly into the cerebellar anlage (arrowheads). (*G*) Sagittal section of postnatal day (P) 3 cerebellar vermis stained with anti-Lmx1a antibody. (*H* and *I*) Higher magnification of the most posterior lobe (boxed region in *G*). At P3, numerous Lmx1a^{+} cells were detected in the posterior vermis. The vast majority of Lmx1a^{+} cells in the internal granule layer (IGL) coexpress the unipolar brush cell (UBC) marker Tbr2. Arrowheads point to several examples of Lmx1a^{+}/Tbr2^{+} cells. The EGL is delineated by the dotted line. (Scale bar: *A*–*C*, 190 μm; *E* and *F*, 100 μm; *G*, 300 μm; *H* and *I*, 90 μm.)

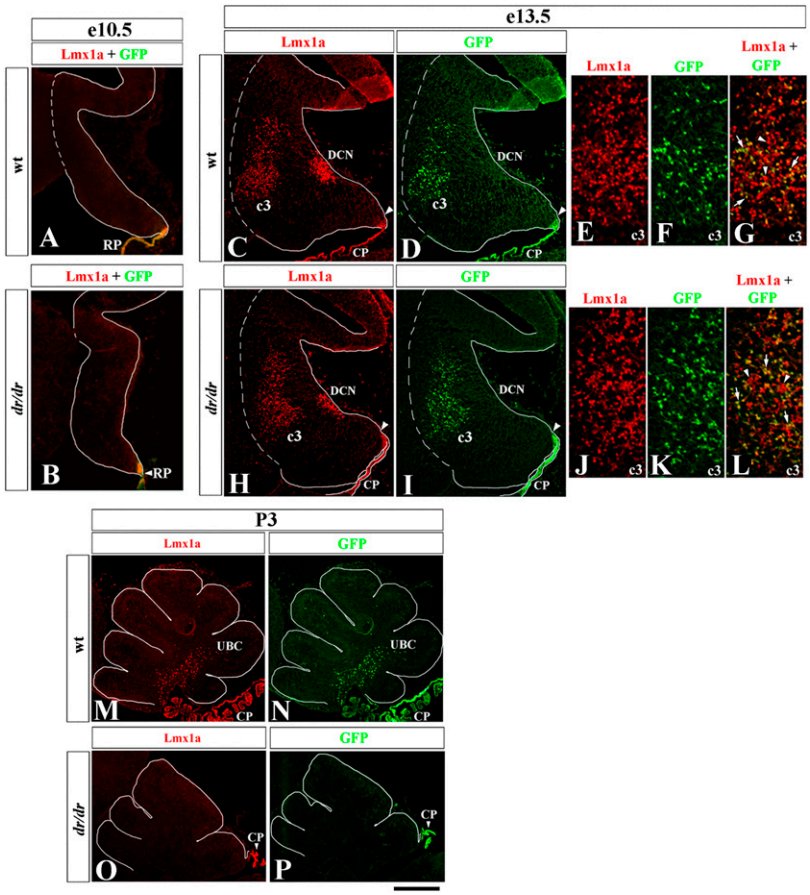

Fig. S2. Analysis of Lmx1a and GFP-Cre expression in wild-type and *dreher Lmx1a-Cre/ROSA* cerebellum. (*A* and *B*) Sagittal sections of cerebellar anlage of e10.5 *Lmx1a-Cre/ROSA* mice on wild-type (*A*) and *dreher* (*dr/dr*) (*B*) background costained with Lmx1a and GFP antibodies. At e10.5, in both wild-type and *dreher* embryos, Lmx1a expression is limited to the fourth ventricle roof plate (RP). GFP-Cre expression faithfully recapitulates Lmx1a expression in both wild-type and *dreher Lmx1a-Cre/ROSA* RP. (*C–L*) Sagittal sections of cerebellar anlage of e13.5 *Lmx1a-Cre/ROSA* mice on wild-type (*C–G*) or *dreher* (*H–L*) background costained with Lmx1a and GFP antibodies. *E–G* and *J–L* show higher magnification of c3 cells. Comparable expression of Lmx1a and GFP-Cre was observed in wild-type and *dreher* embryos. In both wild-type and *dreher* embryos, Lmx1a and EGFP-Cre are coexpressed in CP and RL. Arrowheads in *C*, *D*, *H*, and *I* point to the ventral limit of Lmx1a and GFP-Cre expression in the RL. In addition, in both wild-type and *dreher* embryos, some $Lmx1a^{+}$ c3 cells were GFP^{+} (arrows in *G* and *L*), whereas others were GFP^{-} (arrowheads in *G* and *L*). The same proportion of c3 cells was GFP^{+} in wild-type and *dreher* embryos. In both wild-type and *dreher* embryos, no GFP-Cre expression was detected in deep cerebellar nuclei (DCN) (*D* and *I*). (*M–P*) Sagittal sections of cerebella of P3 *Lmx1a-Cre/ROSA* mice on wild-type (*M* and *N*) and *dreher* (*O* and *P*) background costained with Lmx1a and GFP antibodies. In wild-type cerebellum, Lmx1a and GFP-Cre are expressed in CP and UBC (*M* and *N*). In *dreher* cerebellum, Lmx1a and GFP-Cre are expressed in CP, but they are not expressed in UBC (*O* and *P*). No ectopic expression of GFP-Cre was detected in *dreher* cerebellum. (Scale bar: *A* and *B*, 135 μm; *C*, *D*, *H*, and *I*, 270 μm; *E–G* and *J–L*, 110 μm; *M–P*, 240 μm.)

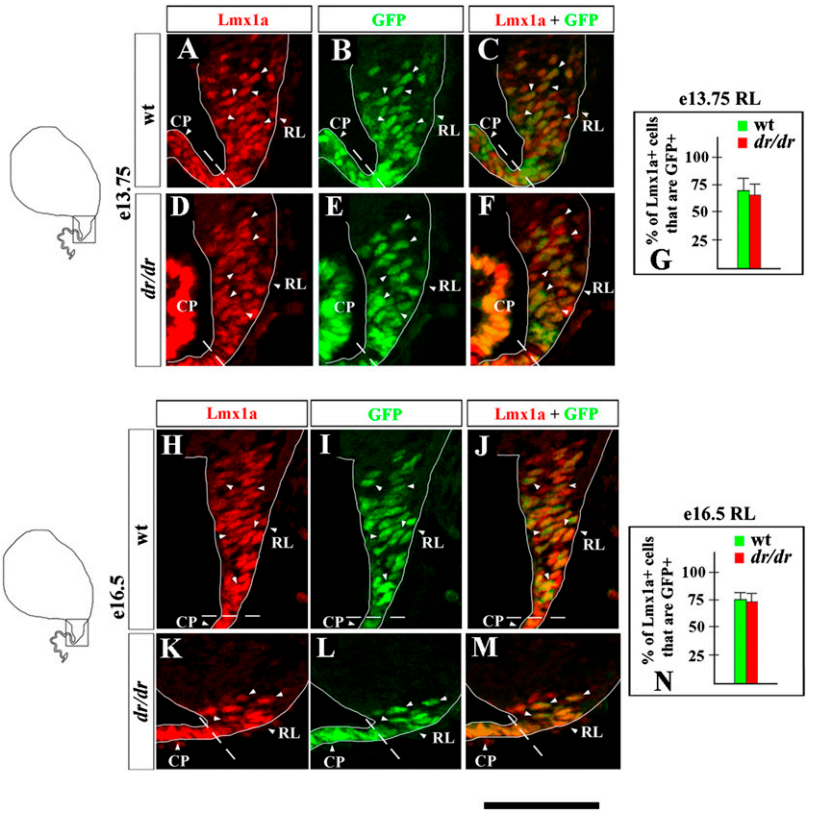

Fig. S3. Detailed analysis of Lmx1a and GFP-Cre expression in wild-type and *dreher Lmx1a-Cre/ROSA* RL. Lmx1a and GFP-Cre expression in wild-type (*A–C* and *H–J*) and *dreher* (*D–F* and *K–M*) *Lmx1a-Cre/ROSA* RL at e13.75 (*A–F*) or e16.5 (*H–M*). In all panels, the area shown (RL and adjacent CP) corresponds to the boxed region in the diagram on the left. Sections are stained with indicated antibodies. Arrowheads point to $Lmx1a^{+}/GFP^{+}$ cells in the RL. In both wild-type and *dreher* RL, the majority of $Lmx1a^{+}$ cells coexpress GFP-Cre. No $GFP^{+}/Lmx1a^{-}$ cells were detected in wild-type or *dreher* RL at either e13.75 or e16.5. (*G* and *N*) Quantification of $Lmx1a^{+}/GFP^{+}$ cells in wild-type and *dreher* RL at e13.75 (*G*) or e16.5 (*N*). Mean ± SD was determined using four embryos of each genotype at each developmental stage. Similar proportions of $Lmx1a^{+}$ cells coexpress GFP in wild-type and *dreher* RL at e13.75 (*G*) and e16.5 (*N*). (Scale bar: 70 μm.)

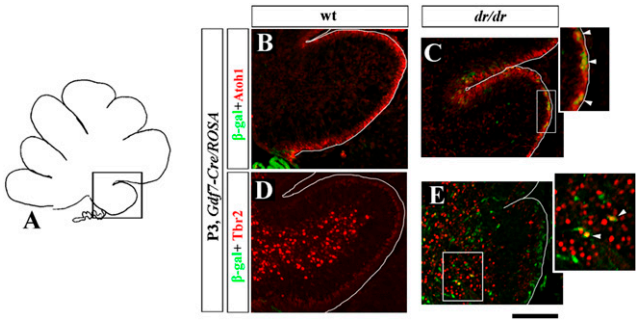

Fig. S4. Contribution of *dreher* RP to posterior vermis granule cells and unipolar brush cells. (*A*) Sagittal section of P3 cerebellar vermis. (*B–E*) Mediolateral sagittal sections of wild-type (*B* and *D*) or *dreher* (*C* and *E*) P3 *Gdf7-Cre/ROSA* cerebella stained with indicated antibodies. The area shown (the most posterior lobe) corresponds to the boxed region in *A*. In wild-type mice, virtually no β-gal staining is present in the cerebellum. In *dreher* mice, some β-gal^{+} cells are present in the EGL (arrowheads in *C Inset*). Atoh1 colabeling indicates that they are granule cells. Some β-gal^{+} cells in *dreher* cerebellum express Tbr2 (arrowheads in *E Inset*), indicating that they adopted the fate of UBCs. (Scale bar: *B–E*, 90 μm; *C* and *E Insets*, 40 μm.)

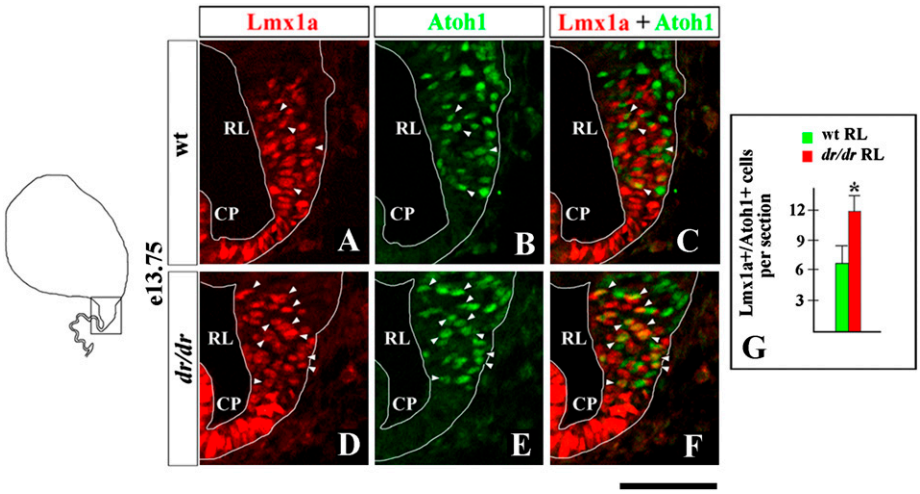

Fig. S5. In *dreher* RL Lmx1a$^+$ cells ectopically express Atoh1. (*A–F*) Sagittal sections of e13.75 wild-type and *dreher* cerebella coimmunostained with Lmx1a and Atoh1. Only RL and adjacent CP (boxed area in the diagram to the left) are shown. Arrowheads point to Lmx1a$^+$/Atoh1$^+$ cells. Many more Lmx1a$^+$ cells coexpress Atoh1$^+$ In *dreher* RL than in wild-type RL. (*G*) Quantification of Lmx1a$^+$/Atoh1$^+$ cells in RL of wild-type (n = 6) and *dreher* (n = 6) embryos. Error bars represent SD. *, $P < 0.01$. (Scale bar: 60 μm.)

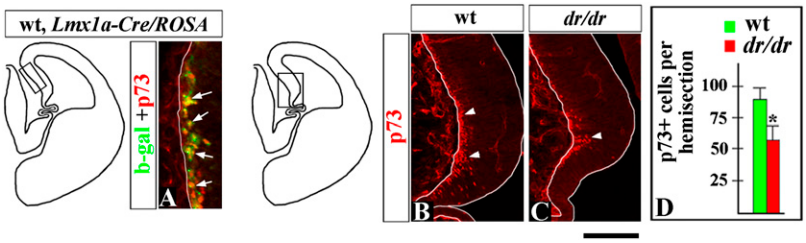

Fig. S6. Lmx1a$^+$ progenitors in the telencephalon give rise to Cajal-Retzius cells, which are reduced in *dreher* embryos. (*A*) Coronal section of e12.5 wild-type *Lmx1a-Cre/ROSA* telencephalon costained with anti–β-gal and p73 antibodies. The area shown corresponds to the boxed region in the diagram to the left. β-Gal$^+$ cells on the pial surface of the developing telencephalon express p73 (arrows) and therefore are Cajal-Retzius cells. (*B* and *C*) p73$^+$ Cajal-Retzius cells (arrowheads) were reduced in e12.5 *dreher* telencephalon. The area shown corresponds to the boxed region in the diagram to the left. (*D*) Quantification of p73$^+$ Cajal-Retzuis cells in wild-type (n = 5) and *dreher* (n = 5) telencephalon at e12.5. Error bars represent SD. *, $P < 0.01$. (Scale bar: *A*, 40 μm; *B* and *C*, 90 μm.)

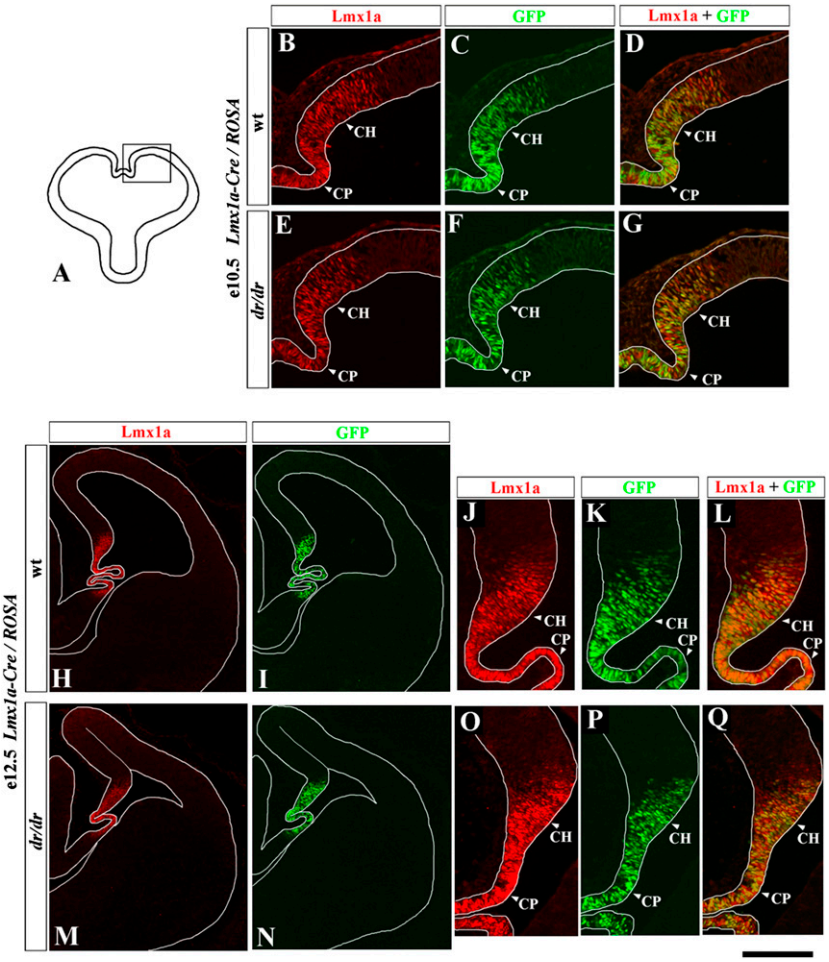

Fig. S7. Analysis of Lmx1a and GFP-Cre expression in the telencephalon of wild-type and *dreher Lmx1a-Cre/ROSA* mice. (*A*) Coronal section of e10.5 telencephalon. (*B–G*) Coronal sections of e10.5 wild-type (*B–D*) or *dreher* (*E–G*) telencephalon stained with indicated antibodies. The area shown in *B–G* corresponds to the boxed region in *A*. Cortical hem (CH) and CP are indicated. Virtually all Lmx1a$^+$ cells in the CP and CH were GFP$^+$ in both wild-type and *dreher* mice at e10.5. (*H–Q*) Coronal sections of e12.5 wild-type (*H–L*) or *dreher* (*M–Q*) telencephalon stained with indicated antibodies. *J–L* and *O–Q* show higher magnifications of CP and CH. Virtually all Lmx1a$^+$ cells in the CP and CH were GFP$^+$ in both wild-type and *dreher* mice at e12.5. No ectopic expression of Lmx1a or GFP-Cre was detected in *dreher* telencephalon. (Scale bar: *B–G*, 100 μm; *H, I, M,* and *N*, 300 μm; *J–L* and *O–Q*, 75 μm.)

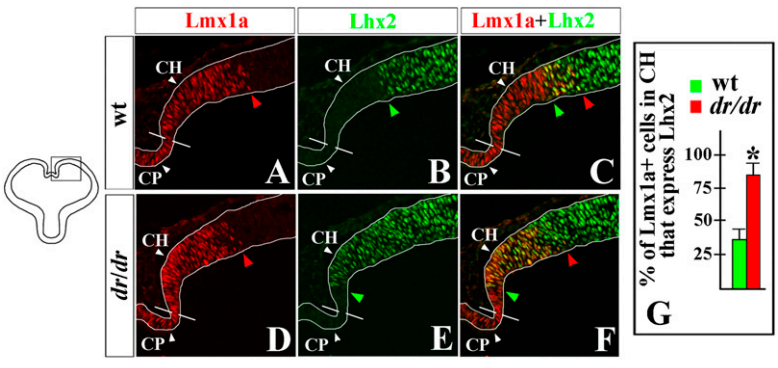

Fig. S8. Ectopic expression of *Lhx2* mediates cell-fate changes in *dreher* CH. (*A–F*) Coronal sections of e10.5 wild-type (*A–C*) or *dreher* (*D–F*) telencephalon stained with indicated antibodies. The area shown corresponds to the boxed area in the diagram to the left. Dashed line marks CP and CH boundaries. Red arrowheads point to the lateral limit of Lmx1a expression; green arrowheads point to the medial limit of Lhx2 expression. In wild-type embryos, Lmx1a and Lhx2 expression domains did not overlap significantly. In *dreher* embryos, Lhx2 expression extended medially and included almost the entire CH (compare *B* and *E*), with significant overlap between Lmx1a and Lhx2 expression domains (compare *C* and *F*). (*G*) Quantification of Lmx1a$^+$/Lhx2$^+$ cells in e10.5 wild-type (n = 5) and *dreher* (n = 6) embryos. A significantly larger fraction of Lmx1a$^+$ cells coexpressed Lhx2 in *dreher* CH than in wild-type CH. Error bars represent SD. *, $P < 0.001$. (Scale bar: 100 μm.)